

# Mechanics of monoclinal systems in the Colorado Plateau during the Laramide orogeny

An Yin

Department of Earth and Space Sciences, University of California, Los Angeles

**Abstract.** Monoclines developed in the Colorado Plateau region during the Laramide orogeny are divided into western and eastern groups by a broad NNW trending antiform through the central part of the plateau. In the western group the major monoclines verge to the east, whereas in the eastern group the major monoclines verge to the west. Paleogeographic reconstruction based on paleocurrent indicators and sedimentary facies distribution suggests that the broad antiform was developed during the Laramide orogeny and was coeval with the formation of the monoclines in the plateau. This relationship implies that the monoclines were drag folds verging towards the center of the plateau as a response to the antiformal warping of the plateau. To simulate the warping of the plateau region and the stress distribution that produced the variable trends of the monoclines, an elastic thin plate model considering in-plane stress was developed. This model assumes that (1) sedimentation in the Laramide basins provided vertical loading along the edge of the plateau region, (2) frictional sliding was operating along the Laramide faults on the northern and eastern boundaries, and (3) the greatest regional compressive stress was oriented in the N60°E direction and was applied uniformly along the western and southwestern sides of the plateau. Buoyancy due to instantaneous isostatic adjustment of crustal thickening or magmatic addition was also considered. The result of the model suggests that the frictional strength of the Uinta thrust system on the northern side of the plateau is at least 2 times greater than that along the Park Range and Sangre de Cristo thrust systems on the eastern side of the plateau in order to explain the observed monoclinial trends and the warping pattern within the plateau during the Laramide orogeny.

## Introduction

### Monoclines in the Colorado Plateau

Monoclines are the principal structures in the Colorado Plateau (Figure 1) [Kelley, 1955a, b; Davis, 1978]. They have various trends (NE, N-S, NW, and E-W) and can be traced from several tens of meters to about 150 km along the strike [Kelley, 1955a, p.794]. Adjacent to the traces of the major monoclines ( $\geq$  tens of kilometers in length) are minor monoclines, folds, and thrusts [e.g., Reches, 1978]. The average shortening strain across the plateau accommodated by the monoclines is estimated at less than 1% [Davis, 1978], although local strains may be much greater. The major monoclines on the plateau, as first noted by Kelley [1955a], can be divided by a NNW trending boundary through the central plateau into a western group in which the monoclines verge to the east and an eastern group in which the monoclines verge to the west (Figure 1).

The kinematic origin of individual monoclines on the plateau has been a subject of investigation since their recognition (see Davis [1978] for references). Kelley [1955a] demonstrated that the monoclines are contractional in origin, because they are commonly associated with minor thrusts and folds. Detailed structural studies on the Kaibab

monocline in Arizona by Reches [1978] and on the Hogback monocline in Colorado by Grout *et al.* [1991] confirmed this interpretation.

The age of the monoclines has been best constrained along the northern and eastern parts of the plateau where the development of the monoclines (e.g., the Uinta monocline, the Hogback monocline, and the Defiance monocline; Figure 1) and the Laramide basins (e.g., the Piceance Creek basin, and the San Juan basin; Figure 1) were intimately related [e.g., Kelley, 1955a; Fassett, 1985; Smith *et al.*, 1985; Grout *et al.*, 1991]. However, the lack of early Tertiary sedimentary rocks, due to either erosion or absence of sedimentation, in the eastern, southern, and central parts of the plateau precludes precise dating of the monoclines in these areas. Because the monoclines on the eastern and southern parts of the plateau (e.g., the Monument and the San Rafael monoclines) involve the Upper Cretaceous sedimentary rocks [King and Beikman, 1974], their formation is likely to be late Cretaceous and early Tertiary during the Laramide orogeny.

### Previous Models

Baker [1935] interpreted that the monoclines were developed under horizontal compression. Kelley [1955a, b] suggested that the variable trends of the monoclines were the result of a complex stress field in which the principal stress directions varied from place to place in the plateau during the Laramide orogeny. Davis [1978] proposed that the variable trends of the monoclines were due to local reactivation of high-angle, preexisting weaknesses in the basement

Copyright 1994 by American Geophysical Union.

Paper number 94JB01408.  
0148-0227/94/94JB-01408\$05.00

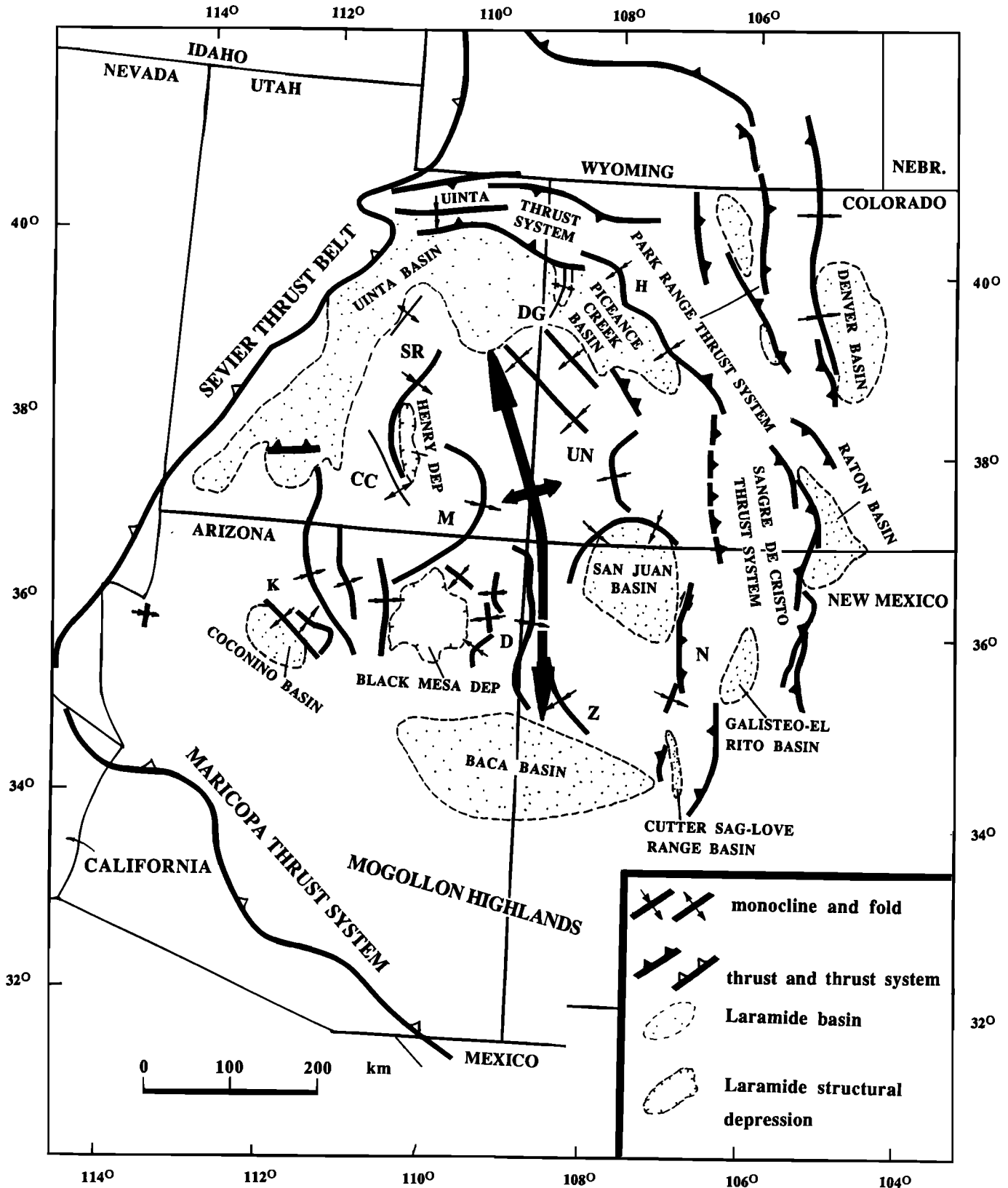


Figure 1. Tectonic map of major monoclines, Laramide faults, and Laramide basins in and adjacent to the Colorado Plateau [after Kelley, 1955a; Davis, 1978; Nation *et al.*, 1985; Lundin, 1989; Merle *et al.*, 1993; and Dickinson *et al.*, 1988]. Major monoclinical systems on the plateau are: K, Kaibab; CC, Circle Cliff; SR, San Rafael; UN, Uncompahgre; DG, Douglas; Z, Zuni; D, Defiance; M, Monument; N, Nacimiento. DEP, structural depression.

in response to regional horizontal compression induced by the interaction between the Farallon and North American plates [e.g., *Coney, 1976; Engebretson et al., 1985*]. Both the Kelley and Davis hypotheses have not been evaluated quantitatively.

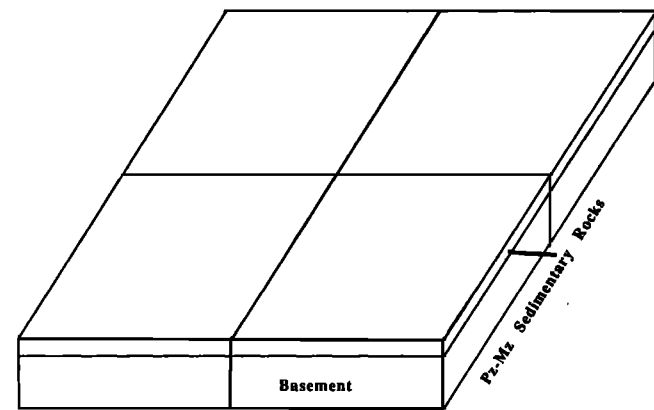
Monoclines are asymmetric folds [*Kelley, 1955a*]. Field observations [*Reches, 1978, p.254*] and theoretical studies [*Reches and Johnson, 1976; Reches and Johnson, 1978*] indicate that the asymmetry can be produced by either the combination of layer-parallel shortening and layer-parallel shearing or the combination of layer-parallel shortening and differential vertical movement along high-angle faults. Although theoretical and experimental works have shown that the relationship between the asymmetry of folds, particularly kink folds, and the sense of bedding-parallel shear is ambiguous [*Reches and Johnson, 1978*], field observations have convincingly demonstrated that many asymmetric folds observed in nature are drag folds associated with flexural-slip folding during the formation of larger folds. This observation suggests that the asymmetrical geometry of drag folds is predictable if the sense of layer-parallel shearing is known [e.g., *Davis, 1985*].

Considering the large area (thousands of square kilometers) in which monoclines have similar vergence (Figure 1), a mechanism that had a regional effect on the monocline asymmetry is implied. The purposes of this paper are (1) to propose a tectonic model that explains both the trend and vergence of the monocline systems as a whole on the plateau, and (2) to present a mechanical model using the elastic thin plate theory that explores the mechanical implications of the proposed tectonic model.

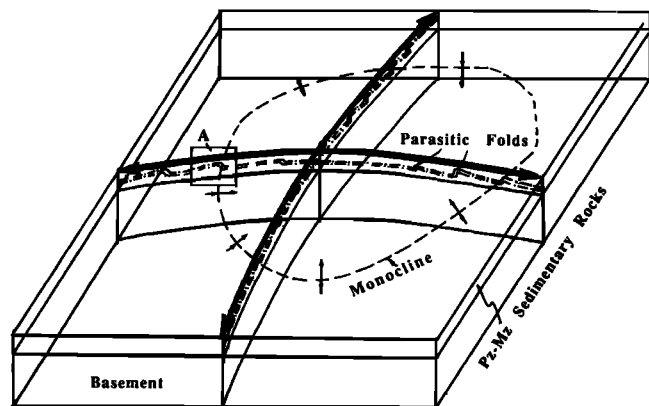
## Tectonic Model

A tectonic model for the development of both the trend and vergence of the monocline systems in the Colorado Plateau region during the Laramide orogeny is proposed here. The Colorado Plateau region was warped from a relatively flat surface into a doubly plunging anticline with its long axis trending north, dividing the eastern and western groups of the monoclines on the plateau (Figures 1 and 2). The warping of the basement crust in the plateau may have caused flexural slip along bedding in the Paleozoic and Mesozoic sedimentary strata on the plateau (Figure 2), reactivation of preexisting weakness, and creation of new fractures that are reverse faults dipping away from the center of the plateau. The sense of flexural slip along bedding according to this hypothesis would have been top-to-the-east on the west side and top-to-the-west on the east side of the plateau (Figure 2). Such a distribution of shear strain in the plateau may have produced monocline systems with the observed trend and vergence (compare Figures 1 and 2).

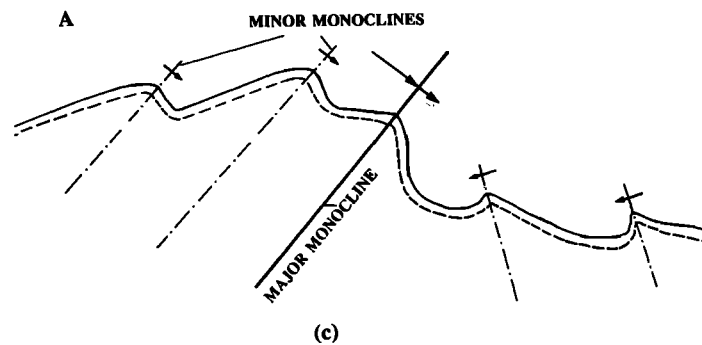
Three pieces of evidence support this proposed model. First, the distribution of Laramide basins along the rim of the plateau suggests that the central plateau was a structural high (Figure 1). Second, paleocurrent directions measured from the Laramide basins around the plateau indicate that the Laramide paleorivers were either flowing along the edge of, or outward from, the plateau [*Ryder et al., 1974; Johnson, 1985; Naton et al., 1985; Smith et al., 1985; Dickinson et al., 1988*]. Third, the basal geometry and isopach patterns of the Laramide basins around the edge of the plateau are asymmetric, deepening away from



(a)



(b)



(c)

**Figure 2.** A three-dimensional tectonic model for the development of the monocline systems in the Colorado Plateau region during the Laramide orogeny. (a) The Colorado Plateau region was assumed to be flat prior to the Laramide deformation. (b) It was warped upward into a broad arch that caused bedding-parallel shearing within the sedimentary strata and the formation of the asymmetric folds verging toward the center of the plateau. (c) Schematic cross section showing relationship between the major monoclines and secondary monoclines and folds as parasitic folds.

the center of the plateau. This pattern is documented, for example, by the variation in thicknesses and sedimentary facies in the Uinta basin: away from the central plateau, sedimentary facies represent deep water conditions, and the

time-equivalent sedimentary sequences are thicker [Johnson, 1985].

The inferred domal arching of the Colorado Plateau during the Laramide orogeny may not mean that the plateau was topographically higher than the surrounding areas immediately outside the plateau (i.e., the Sevier thrust belt to the west and the Rocky Mountains to the east). In fact, the suggested domal anticline in the plateau could have been topographically lower than the surrounding marginal regions. A modern analogue to the paleotectonic and paleogeographic settings of the Colorado Plateau during the Laramide orogeny is the Tarim basin in northwestern China. Although the altitude of the basin is lower than its surrounding mountain ranges (i.e., the Tibetan Plateau to the south and the Tian Shan Mountains to the north), the basement of the basin itself is a broad anticline which is defined by thickening of the late Tertiary sections up to 7 km thick toward the rim of the Tarim basin [e.g., Wang *et al.*, 1992].

## Mechanical Model

The proposed tectonic model leads to questions about what caused the domal warping of the plateau (e.g., buckling by horizontal compression, bending by vertical load, or a combination of both) and what mechanical conditions were in existence along the boundaries of the plateau (sides and the base) that led to the domal warping and variable trends of the monoclines. To address these questions, an elastic thin-plate model is presented that examines the interactions among: (1) the loading along the edge of the plateau due to Laramide thrusting and sedimentation; (2) the horizontal compression due to interaction of the Farallon and the North American plates; (3) frictional sliding along the Laramide faults on the northern and eastern boundaries of the plateau; and (4) the buoyancy effect beneath the plateau due to protracted magmatic underplating and crustal thickening at the base of the plateau during the Laramide orogeny. The Colorado Plateau may have generally been in an isostatic equilibrium during the duration of the Laramide orogeny. It is conceivable, however, that magmatic addition at the base of the crust would have caused short-term isostatic adjustments, as the density structure of the plateau region was perturbed. Consequently, an upward push of the brittle-elastic upper crust would have occurred, although this force may have only been in existence for a short time. The purpose of the following numerical simulation is to treat all of the above features as related products of a single mechanical system. In particular, the numerical simulation uses the monoclinical trends and the domal warping pattern of the Colorado Plateau as constraints to determine the mechanical conditions along the sides of the plateau.

The Colorado Plateau as used in this study does not refer to the present physiographic feature. Instead, it is the region that existed during the early Tertiary and was only mildly deformed during the Laramide orogeny and is bounded by the Sevier thrust belt to the west, the Maricopa thrust system to the southwest, the Uinta Mountains thrust to the north, the Park Range thrust to the northeast, and the Sangre de Cristo thrust to the southeast (Figure 1). The Colorado Plateau of the early Tertiary was somewhat larger than its present extent and had a different geometry, because the late Cenozoic extension may have reduced the size of the plateau [e.g., Wernicke, 1985].

## Governing Equations

Because the overall shortening strain accommodated by the monoclines across the plateau is less than 1%, the deformation of the plateau during the Laramide orogeny may be best modeled as a thin elastic plate. Although *Beaumont* [1981] and *Quinlin and Beaumont* [1984] suggested that flexure of the lithosphere behaves viscoelastically, studies by *Jordan* [1981] and *Sinclair et al.* [1991] showed that elastic thin plate models can be equally successful in interpreting the history of foreland basin development. As the warping of the plateau may have been related to loading caused by the sedimentation in the Laramide basins (which was completed in a duration of 20-40 m.y.), we need to consider the incremental warping of the plateau at each stage and sum them to obtain the overall pattern of the warping at the end of the Laramide orogeny. Let us consider a right-handed rectangular Cartesian frame of reference with the  $xy$  plane coinciding with the middle plane of a thin plate and the  $z$  axis normal to it (Figure 3a). Normal and shear stress components in the  $x$ ,  $y$ , and  $z$  directions are shown in Figures 3b and 3c. The sign convention in the calculations follows that of elasticity, that is, tensile stress is positive. The governing equation for deflection of a thin elastic plate due to combined vertical and horizontal forces in three dimensions [e.g., *Fung*, 1965] is

$$\begin{aligned} \frac{\partial^4 w}{\partial x^4} + 2\frac{\partial^4 w}{\partial x^2 \partial y^2} + \frac{\partial^4 w}{\partial y^4} = \frac{1}{D}[q(x, y) \\ + N_x(x, y)\frac{\partial^2(w_0 + w)}{\partial x^2} + 2N_{xy}(x, y)\frac{\partial^2(w_0 + w)}{\partial x \partial y} \\ + N_y(x, y)\frac{\partial^2(w_0 + w)}{\partial y^2}] \end{aligned} \quad (1)$$

where  $w_0$  is the initial deflection of the plate,  $w$  is the deflection normal to the  $xy$  plane under a set of boundary conditions which is discussed below, and  $q(x, y)$  is the distribution of vertical load. If the vertical load is due to an instantaneous isostatic adjustment caused by either erosion or magmatic addition to the crust, then  $q(x, y)$  may be calculated by

$$q(x, y) = (\rho_m - \rho_c)gr(x, y) \quad (2)$$

where  $g$  is the gravitational acceleration,  $r(x, y)$  represents the shape of the crustal root to be adjusted isostatically (Figure 4), and  $\rho_m$  and  $\rho_c$  are the average densities of the mantle and crust.  $D$  is the flexural rigidity defined by

$$D = \frac{Eh^3}{12(1 - \nu^2)} \quad (3)$$

where  $h$  is the thickness of the elastic plate,  $E$  is Young's modulus, and  $\nu$  is Poisson's ratio; the terms  $N_x(x, y)$ ,  $N_y(x, y)$ , and  $N_{xy}(x, y)$  (forces per unit length) in equation (1) are the normal and shear stress resultants in the  $x$  and  $y$  directions acting on the middle plane  $z = 0$  of the thin plate (Figure 3b). They are related to the stress components by

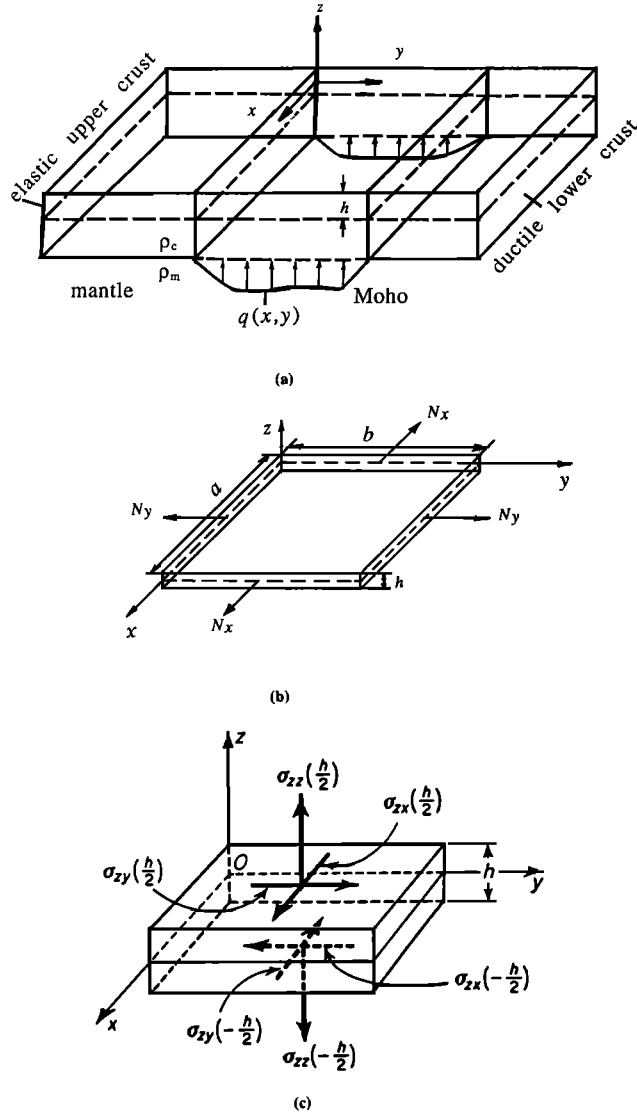


**Figure 3.** Notation of external loads, stress components, and framework of reference. (a) Coordinate system used in the computation. The origin is located on the middle surface of the assumed elastic thin plate.  $h$  is the thickness of the plate;  $q(x, y)$  is the vertical force due to uncompensated crustal root;  $\rho_c$  and  $\rho_m$  are the densities of the crust and mantle, respectively. (b) Stress resultants  $N_x$  and  $N_y$  as defined in the text in the  $x$  and  $y$  directions. (c) Normal and shear stress components on the top and base of the plate. Note that we assume  $\sigma_{xy}(h/2) = \sigma_{xy}(-h/2) = \sigma_{zx}(h/2) = \sigma_{zx}(-h/2) = 0$  in the computation.

$$\begin{aligned}
 N_x(x, y) &= \int_{-h/2}^{h/2} [\sigma_{xx}(x, y, z) - \sigma_{zz}(x, y, z)] dz \\
 &= h \left[ \frac{1}{h} \int_{-h/2}^{h/2} \sigma_{xx}(x, y, z) dz \right. \\
 &\quad \left. - \frac{1}{h} \int_{-h/2}^{h/2} \sigma_{zz}(x, y, z) dz \right] \\
 &= h[\bar{\sigma}_{xx}(x, y) - \bar{\sigma}_{zz}(x, y)] \quad (4a)
 \end{aligned}$$

$$\begin{aligned}
 N_y(x, y) &= \int_{-h/2}^{h/2} [\sigma_{yy}(x, y, z) - \sigma_{zz}(x, y, z)] dz \\
 &= h \left[ \frac{1}{h} \int_{-h/2}^{h/2} \sigma_{yy}(x, y, z) dz \right. \\
 &\quad \left. - \frac{1}{h} \int_{-h/2}^{h/2} \sigma_{zz}(x, y, z) dz \right] \\
 &= h[\bar{\sigma}_{yy}(x, y) - \bar{\sigma}_{zz}(x, y)] \quad (4b)
 \end{aligned}$$

$$\begin{aligned}
 N_{xy}(x, y) &= \int_{-h/2}^{h/2} \sigma_{xy}(x, y, z) dz \\
 &= h\bar{\sigma}_{xy}(x, y), \quad (4c)
 \end{aligned}$$

where  $\sigma_{xx}(x, y, z)$ ,  $\sigma_{yy}(x, y, z)$ , and  $\sigma_{zz}(x, y, z)$  are normal stress components in the  $x$ ,  $y$ , and  $z$  directions, and  $\bar{\sigma}_{xx}$ ,  $\bar{\sigma}_{yy}$ , and  $\bar{\sigma}_{zz}$  are their averaged values integrated vertically;  $\sigma_{xy}$  is the shear stress component in the  $x$  and  $y$  directions on the  $xz$  and  $yz$  planes, and  $\bar{\sigma}_{xy}$  is its vertically averaged value. Stress resultants  $N_x$  and  $N_y$  are so defined in (4a) and (4b) that the influence of lithostatic stresses is removed and that the deflection  $w$  defined in (1) is produced only by tectonically induced deviatoric stresses.

The stress components  $\bar{\sigma}_{xx}$ ,  $\bar{\sigma}_{yy}$ , and  $\bar{\sigma}_{xy}$  on the horizontal plane are governed by the stress equilibrium equations

$$\frac{\partial^2 \bar{\sigma}_{xx}}{\partial x^2} + \frac{\partial^2 \bar{\sigma}_{xy}}{\partial y^2} = 0 \quad (5a)$$

$$\frac{\partial^2 \bar{\sigma}_{xy}}{\partial x^2} + \frac{\partial^2 \bar{\sigma}_{yy}}{\partial y^2} = 0. \quad (5b)$$

Equations (5a) and (5b) can be calculated by the Airy-stress-function method [Fung, 1965], i.e.,

$$\bar{\sigma}_{xx} = \frac{\partial^2 \phi}{\partial y^2} \quad (6a)$$

$$\bar{\sigma}_{yy} = \frac{\partial^2 \phi}{\partial x^2} \quad (6b)$$

$$\bar{\sigma}_{xy} = -\frac{\partial^2 \phi}{\partial x \partial y} \quad (6c)$$

where  $\phi$  is the Airy stress function that satisfies the biharmonic equation

$$\frac{\partial^4 \phi}{\partial x^4} + 2 \frac{\partial^4 \phi}{\partial x^2 \partial y^2} + \frac{\partial^4 \phi}{\partial y^4} = 0. \quad (6d)$$

For a given set of boundary conditions, (6) can be solved, and thus the stress distribution of  $\bar{\sigma}_{xx}$ ,  $\bar{\sigma}_{xy}$ , and  $\bar{\sigma}_{yy}$  and the stress resultants  $N_x(x, y)$ ,  $N_y(x, y)$ , and  $N_{xy}(x, y)$  are determined. Once  $N_x(x, y)$ ,  $N_y(x, y)$ , and  $N_{xy}(x, y)$  are known, we can solve (1) to obtain  $w(x, y)$ , which shows the warping pattern of the plateau.

### Boundary Conditions

To simulate the stress distribution and the warping pattern in the Colorado Plateau region during the Laramide orogeny, either traction or displacement boundary conditions along the edge and base of the plateau need to be defined. We assume that the compressive traction with a uniform direction and a constant magnitude was applied along the northwestern and southwestern sides of the plateau. The

traction, decomposed into shear and normal components, was transmitted across the plateau and was balanced by friction along the Laramide faults on the eastern and northern sides of the plateau (Figure 4).

Before considering the boundary conditions along the edge of the Colorado Plateau, it is important to know the state of the regional stress at the edge of the plateau. The principal stress direction may be inferred from reconstruction of plate kinematics [e.g., *Engelbreton et al.*, 1985]. The stress magnitude is difficult to estimate. However, it is believed to vary in a limited range between 10 and 100 MPa [see *Mount and Suppe*, 1992, and references therein].

Because there were no major Laramide faults developed along the northwestern and southwestern sides of the plateau during the Laramide orogeny, the assumed stress state along the boundary is the same as that of the regional stress with the greatest compressive direction in N60°E. Assuming that the vertical normal stress  $\sigma_{zz}$  is lithostatic along the southwestern and northwestern sides of the plateau (sides 1 and 2 in Figure 4), i.e.,  $\sigma_{zz}^i = -\rho g[(h/2) - z]$ , its vertical average is  $\bar{\sigma}_{zz}^i = -\frac{1}{2}\rho_c g h$ , where  $i = 1, 2$ . We further assume that the vertically averaged horizontal principal stresses  $\bar{\sigma}_1^i$  and  $\bar{\sigma}_2^i$  are uniformly applied on each of the two sides. We obtain

$$s\bar{\sigma}_1 = t\bar{\sigma}_2 = \bar{\sigma}_{zz} = -\rho_c g \frac{h}{2} \quad (7a)$$

$$\bar{\sigma}_1 = \alpha \bar{\sigma}_{zz} \quad (7b)$$

$$\bar{\sigma}_2 = \beta \bar{\sigma}_{zz} \quad (7c)$$

where  $s, t, \alpha$  and  $\beta$  are constants. Using (4a), (4b), (4c), (7a), (7b), and (7c) and noting that

$$\bar{\sigma}_{xx} = \frac{1}{2}(\bar{\sigma}_1 + \bar{\sigma}_2) + \frac{1}{2}(\bar{\sigma}_1 - \bar{\sigma}_2) \cos 2\theta \quad (8a)$$

$$\bar{\sigma}_{yy} = \frac{1}{2}(\bar{\sigma}_1 + \bar{\sigma}_2) + \frac{1}{2}(\bar{\sigma}_1 - \bar{\sigma}_2) \cos(2\theta + \frac{\pi}{2}) \quad (8b)$$

$$\bar{\sigma}_{xy} = \frac{1}{2}(\bar{\sigma}_1 - \bar{\sigma}_2) \sin 2\theta \quad (8c)$$

we can determine  $N_x, N_y$ , and  $N_{xy}$ .  $\theta$  in (8a), (8b), and (8c) is the angle between  $\bar{\sigma}_1$  and  $\bar{\sigma}_{xx}$ . Without tectonic disturbance, the lithosphere is under lithostatic stress, that is,

$$\bar{\sigma}_{xx} = \bar{\sigma}_{yy} = \bar{\sigma}_{zz} = -\frac{1}{2}\rho_c g h \quad (9a)$$

$$N_x = N_y = N_z = 0. \quad (9b)$$

The boundary condition along the northern (the Uinta Mountain fault system, side 5 of Figure 4), northeastern (the Park Range thrust system, side 4 of Figure 4), and

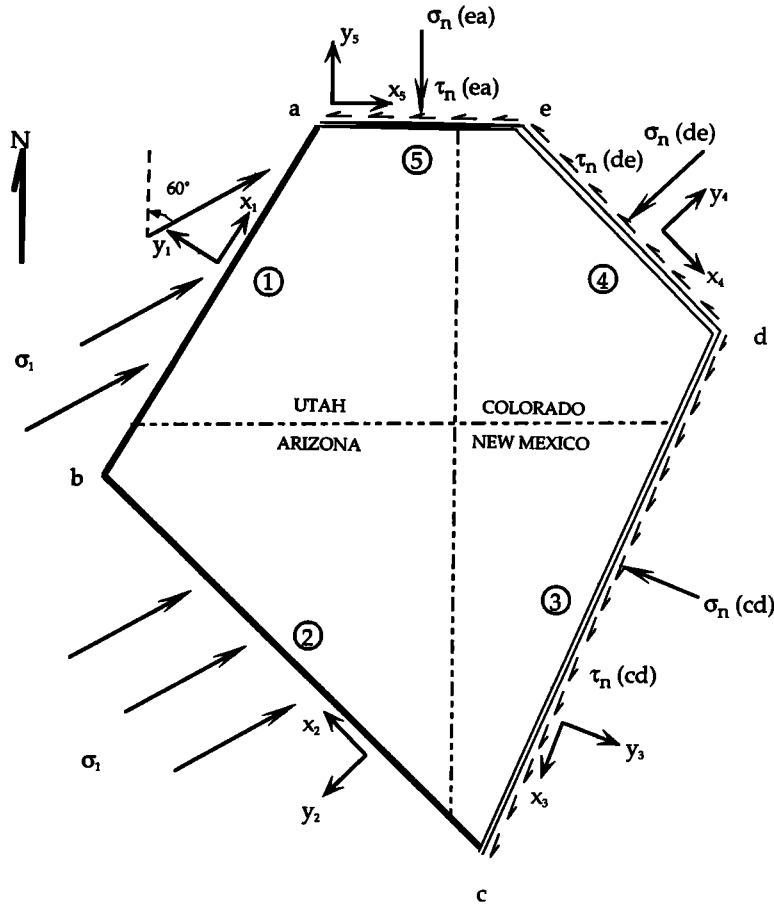


**Figure 4.** The geometry of the model, local coordinate systems, and the forces applied along the boundaries.  $\sigma_1$  represents the greatest compressive direction applied along the northwestern and southwestern sides of the plate.  $\tau_n$  and  $\sigma_n$  are shear and normal tractions on sides cd, de, and ea, which define the traction boundary conditions along the northern and eastern sides. Circled numbers refer to each side, i.e., 1 = ab, 2 = bc, 3 = cd, 4 = de, and 5 = ea.

southeastern (the Sangre de Cristo thrust system, side 3 of Figure 4) boundaries of the plateau are assumed to be governed by frictional sliding following the Amonton law [Jaeger and Cook, 1979], i.e.,

$$\bar{\tau}_n^i = \mu^i (1 - \lambda^i) \bar{\sigma}_n^i \quad (10)$$

where  $i = 3, 4$ , and  $5$ ,  $\bar{\sigma}_n^i$  and  $\bar{\tau}_n^i$  are the vertically averaged normal and shear tractions on each fault surface,  $\mu^i$  is the coefficient of friction along the fault, and  $\lambda^i$  is the pore-fluid pressure ratio of Hubbert and Rubey [1959]. In the following calculation, we use  $\mu_e^i = \mu^i (1 - \lambda)$  to represent the effective coefficient of friction.

The six unknown stress components along sides 3, 4, and 5 of the plateau (Figure 4) can be determined using six equations: three are defined in (10) and the additional three are obtained by balancing forces and torques along the boundary of the plateau, i.e.,

$$\Sigma F_x = \Sigma F_y = \Sigma M = 0 \quad (11)$$

where  $F_x$  and  $F_y$  are tractions applied in the  $x$  and  $y$  directions and  $M$  is the torque applied on the boundary of the plateau.

Lithospheric flexure during the development of foreland basins may be due to thrusting and sediment loading [e.g., Jordan, 1981]. The thrust load can be calculated by constructing accurate cross sections with consideration of erosion. The sediment load can be calculated from the known thickness of the sedimentary strata at a certain time interval. This may be done for the boundary conditions along the northern boundary in the Uinta Mountains, the northeastern boundary in the Park Range, and the southeastern boundary in the Nacimiento uplift. As suggested by Yin and Ingersoll [1993], motion along the Uinta Mountains thrust, the Park Range thrust, and the Nacimiento-Sangre de Cristo thrust system may have led to the development of the Uinta, Piceance Creek, and San Juan basins (Figure 1). We treat these sides as simply supported in the  $x$  and  $y$  directions. This requires

$$\frac{\partial^2 w}{\partial x_i^2} = 0 \quad (12a)$$

$$\frac{\partial^2 w}{\partial y_i^2} = 0 \quad (12b)$$

where  $x_i, y_i$  are right-handed local coordinates and are normal and parallel to the boundary of the plateau (Figure 4). However, as the thrust load has been eroded away since the Laramide orogeny, it is difficult to obtain information regarding the exact magnitude of thrust loading during the warping of the plateau. Thus I assume that the thickness of the Laramide basin sediments equals the magnitude of deflection along the edge of the plateau, i.e.,

$$w_i = T_i, i = 1, 2, 3, 4, 5, \quad (13)$$

where  $w_i$  is deflection along each of the five sides of the plateau (Figure 4) and  $T_i$  is the thickness of the sediments in the Laramide basins (e.g., the Uinta, Piceance Creek, and San Juan basins). Because the thickness of the Laramide basin sediments varies, the greatest thickness, near the out-

ermost part of the plateau region, is used for the deflection boundary condition.

In contrast to the northern, northeastern, and southeastern boundaries of the plateau, the southwestern side of the plateau (i.e.,  $i = 4$ ) probably remained at the same elevation or was slightly uplifted during the Laramide orogeny to form the Mogollon Highlands (Figure 1), which in turn were probably produced by the movement along the southwest directed Maricopa thrust system dipping towards the plateau [Nation et al., 1985]. Thus, instead of subsiding during the Laramide orogeny, the southwest edge of the plateau was probably uplifted with respect to the central part of the plateau. Because it is difficult to estimate quantitatively the amount and history of the uplift, the magnitude of deflection along this side is somewhat uncertain. Laramide age thrusts along the northwestern side of the plateau in southern Nevada and southeastern California are rare, if they existed at all, because thrusts there were intruded by late Cretaceous plutons [e.g., Burchfiel and Davis, 1981; Fletcher and Karlstrom, 1990]. Because the Sevier thrust belt is mostly active between the Early to Middle Cretaceous, its development predates the Laramide orogeny as well as the formation of the monoclinical systems on the Colorado plateau. However, the presence of the Uinta basin along this boundary (Figure 1) suggests that this side of the plateau was deflected downward during the development of the monoclines.

## Calculation Procedure

Figure 5 is a flowchart showing the sequence of calculations for this study. Traction boundary conditions were used to solve the in plane stress distribution, i.e.,  $\bar{\sigma}_{xx}(x, y)$ ,  $\bar{\sigma}_{yy}(x, y)$ , and  $\bar{\sigma}_{xy}(x, y)$ . This was done by solving equation (6) using an explicit finite difference method. We then input deflection boundary conditions  $w_i$ ,  $w_i$ ,  $w_i$  sequentially along each side of the plateau to calculate the deflection pattern  $w(x, y)$  by solving equation (1), and again by using the explicit finite-difference method. The computer code was tested in simple conditions under which analytical solutions are known. The match of the two is excellent.

## Selection of Parameters

There are 8 parameters,  $\alpha_1, \alpha_2, \beta_1, \beta_2, \mu_e^3, \mu_e^4, \mu_e^5$ , and  $h$ , deciding the stress distribution in the thin plate, plus 14 parameters,  $\alpha_1, \alpha_2, \beta_1, \beta_2, \mu_e^3, \mu_e^4, \mu_e^5, h, r, w_1, w_2, w_3, w_4$ , and  $w_5$ , deciding the deflection pattern of the thin plate. The number of combinations of these parameters is large. If we consider that the upper crust and the upper mantle of the lithosphere are decoupled by the ductile lower crust, we can assume that the elastic thickness of the thin plate is less than 20 km. That  $\beta_1 = \beta_2 = 1.0$  implies no compressional deviatoric stress perpendicular to the regional maximum compressional direction. In this case, assuming  $\alpha_1 = \alpha_2 = 1.1$  is equivalent to prescribing the magnitude of horizontal deviatoric stress  $(\bar{\sigma}_1 - \bar{\sigma}_2) = 21$  MPa, and assuming  $\alpha_1 = \alpha_2 = 1.5$  is equivalent to prescribing the magnitude of horizontal deviatoric stress  $(\bar{\sigma}_1 - \bar{\sigma}_2) = 150$  MPa. The range of coefficients of friction based on experimental mechanics is between 0.3 and 1.2 [Byerlee, 1978]. The deflection along the edge of the plateau during the Laramide orogeny is no more than 3 km, because the thicknesses of the Laramide basins along the northern and eastern rim of the

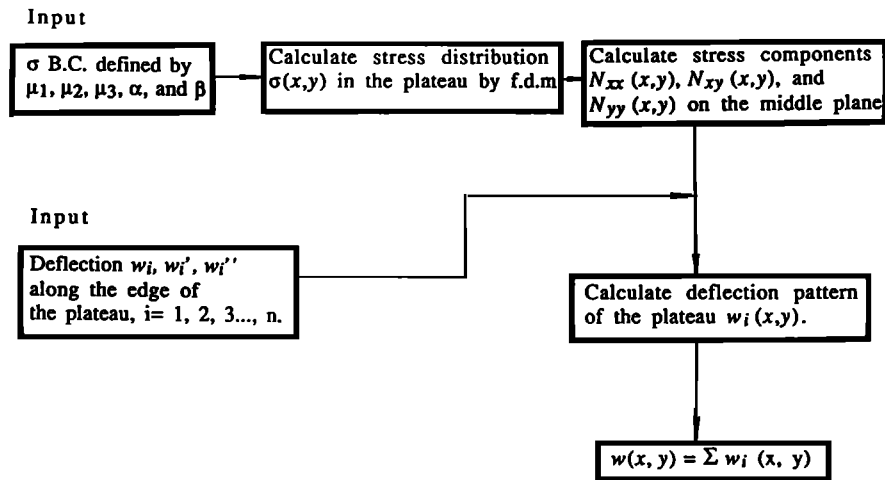


Figure 5. Flowchart showing the computation procedure for determining the stress distribution and deflection pattern. Symbols in the chart are: B.C., boundary conditions; f.d.m., finite difference method.

plateau range from several hundreds of meters to at most 3.5 km [Dickinson *et al.*, 1988].

### Criteria for Best Fit Simulations

The requirements for a best fit simulation are that (1) it predicts the greatest compressive direction perpendicular to the trends of the major monoclines; (2) it produces a broad N-S trending arch in the central plateau with a magnitude of deflection no greater than 5 km with respect to the deepest part of the simulated basins; (3) it produces the foreland basins along the northern and eastern sides of the plateau; (4) the average magnitude of the deviatoric stress is between 20 and 100 MPa, and (5) it predicts simultaneous N-S compression near the northern boundary and E-W compression near the eastern boundary.

Instead of setting up an automated program to search for the best fit simulations, a systematic evaluation of parameters within reasonable limits was conducted. This approach allows us to explore the physics of the investigated mechanical system; that is, we learn from the simulations of not only the successful runs but also from those that failed to explain the observations.

## Results and Discussion

### Best Fit Simulation

Although there are a total of 22 parameters, we find that only a very few of the simulations satisfy all the criteria and the limited range of each parameter discussed above. After systematically evaluating each of the parameters with about 100 computer runs in total, the best fit simulation is shown in Figure 6. In this computation, we assume that  $\mu_e^3 = \mu_e^4 = 0.40$ ,  $\mu_e^5 = -1.00$ ,  $\alpha_1 = \alpha_2 = 1.1$ , and  $\beta_1 = \beta_2 = 1.0$ . We assume that the northern, northeastern, northwestern, and southeastern edges of the plateau region were deflected downward 1.5 km due to basin loading, i.e.,  $w_1 = w_3 = w_4 = w_5 = -1.5$  km. This value is less than the maximum thickness of the Laramide sediments around the rim of the plateau (e.g., 2 km for the Uinta basin, see Ryder *et al.* [1974]; also see Dickinson *et al.* [1988]).

However, as the deflection is not uniform along the strike on each side of the plateau, an average value of 1.5 km is taken to approximate the overall deflection boundary conditions. The magnitude of deflection along the southwestern edge of the plateau is assumed to be zero, because there are no Laramide basins developed along this edge. Thus this area might have had an upward deflection due to uplift associated with northeast dipping the Maricopa thrust system (Figure 1). In the computation shown in Figure 6, we assumed that  $w_2 = 0.0$ , because  $w_2$  between 0.0 and 1.0 km produces essentially the same deflection pattern with a slight change in the magnitude of deflection. The effective elastic thickness of the plateau is assumed to be  $h = 10$  km, which provides a relatively good fit in both stress and deflection magnitudes. The uncompensated crustal root is assumed to be  $r = 0.5$  km. We find that this value must be kept smaller than 2 km in order to have the deflection magnitude in the range of several kilometers. Note that  $\mu_e^i = 0$  is equivalent to assuming dip-slip faulting. The sign in front of the coefficient of friction indicates the sense of horizontal slip along these bounding faults: a negative sign indicates that the fault block outside the plateau region moves in an opposite direction to the local positive direction of the  $x$  axis (Figure 4).

The calculated principal stress trajectories are superimposed on the geologic map (Figure 7). The predicted greatest compressive principal stress direction is, in general, perpendicular to most of the monoclinical systems in the plateau region. The fit is excellent along the northern, eastern, and southwestern boundaries. The stress pattern is consistent with the observation that the northern, eastern, and southwestern boundaries of the plateau were all under compression during the Laramide orogeny. Surface mapping [Hansen, 1965], subsurface seismic and drill hole data [Gries, 1983], and detailed kinematic studies [Bernaski, 1985] in the Uinta Mountains area suggest that the principal compressional direction during the Laramide orogeny is nearly north-south. Similarly, the stress pattern is consistent with dominant thrusting during the Laramide orogeny along the eastern side (see summary by Dickinson *et al.* [1988]) [cf. Chapin and Cather, 1983] and the southwestern side of the plateau [Drewes, 1988]. Right-slip faults are

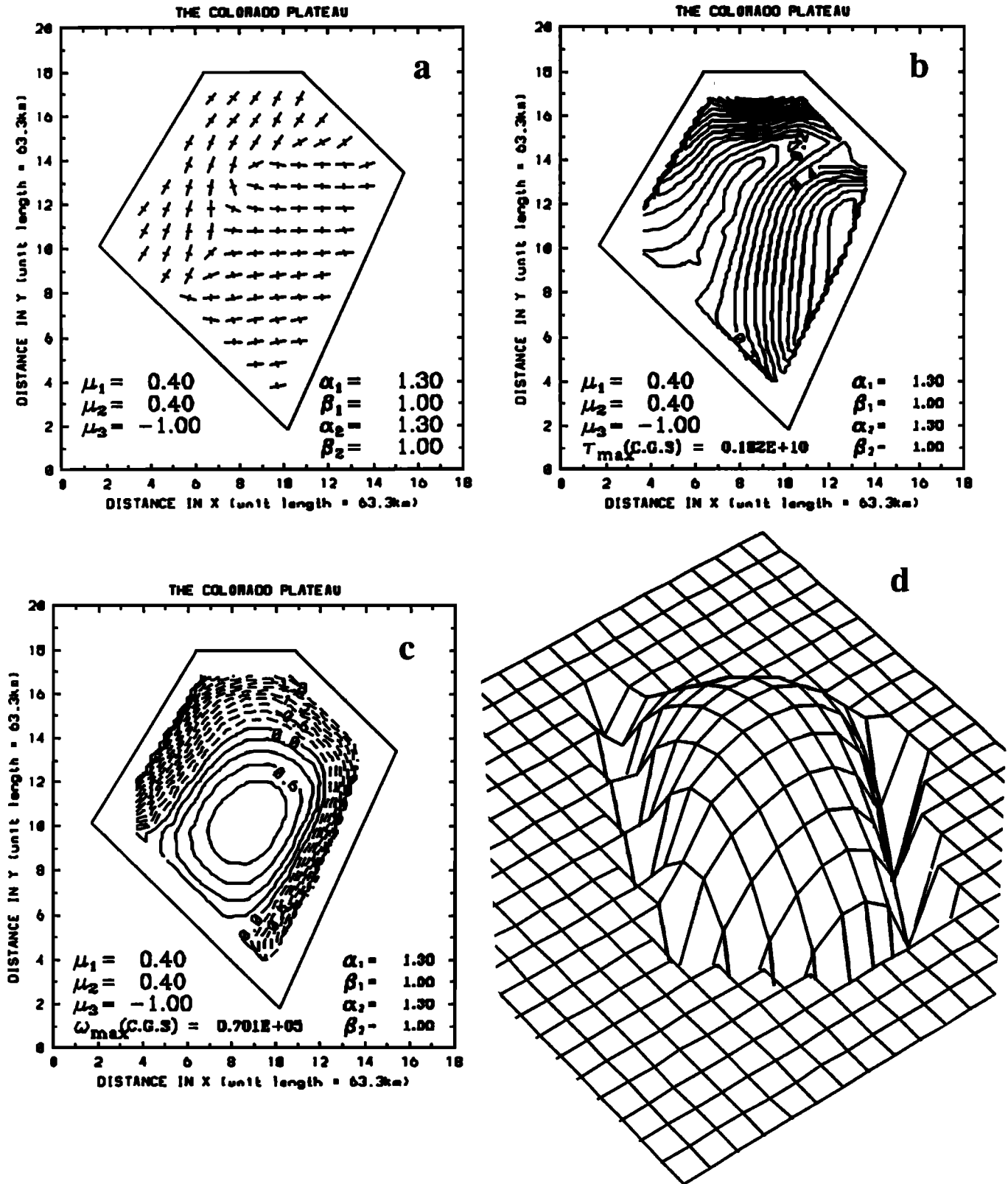


Figure 6. The best-fit simulation model of the Colorado Plateau. (a) Directions of the principal stresses (long dashes show the maximum compressive stress direction, and short transverse dashes show the minimum compressive stress direction), (b) the magnitude of deviatoric stress, and (c) and (d) the deflection pattern of the thin plate. The effective coefficient of friction along the northern boundary fault (the Uinta thrust system) is assumed to be  $\mu_e^5 = -1.00$ . Other parameters are  $h = 10$  km,  $r = 0.5$  km,  $\mu_e^3 = \mu_e^4 = 0.4$ ,  $\alpha_1 = \alpha_2 = 1.1$ ,  $\beta_1 = \beta_2 = 1.0$ ,  $w_2 = 0$ , and  $w_1 = w_3 = w_4 = w_5 = -1.5$  km.

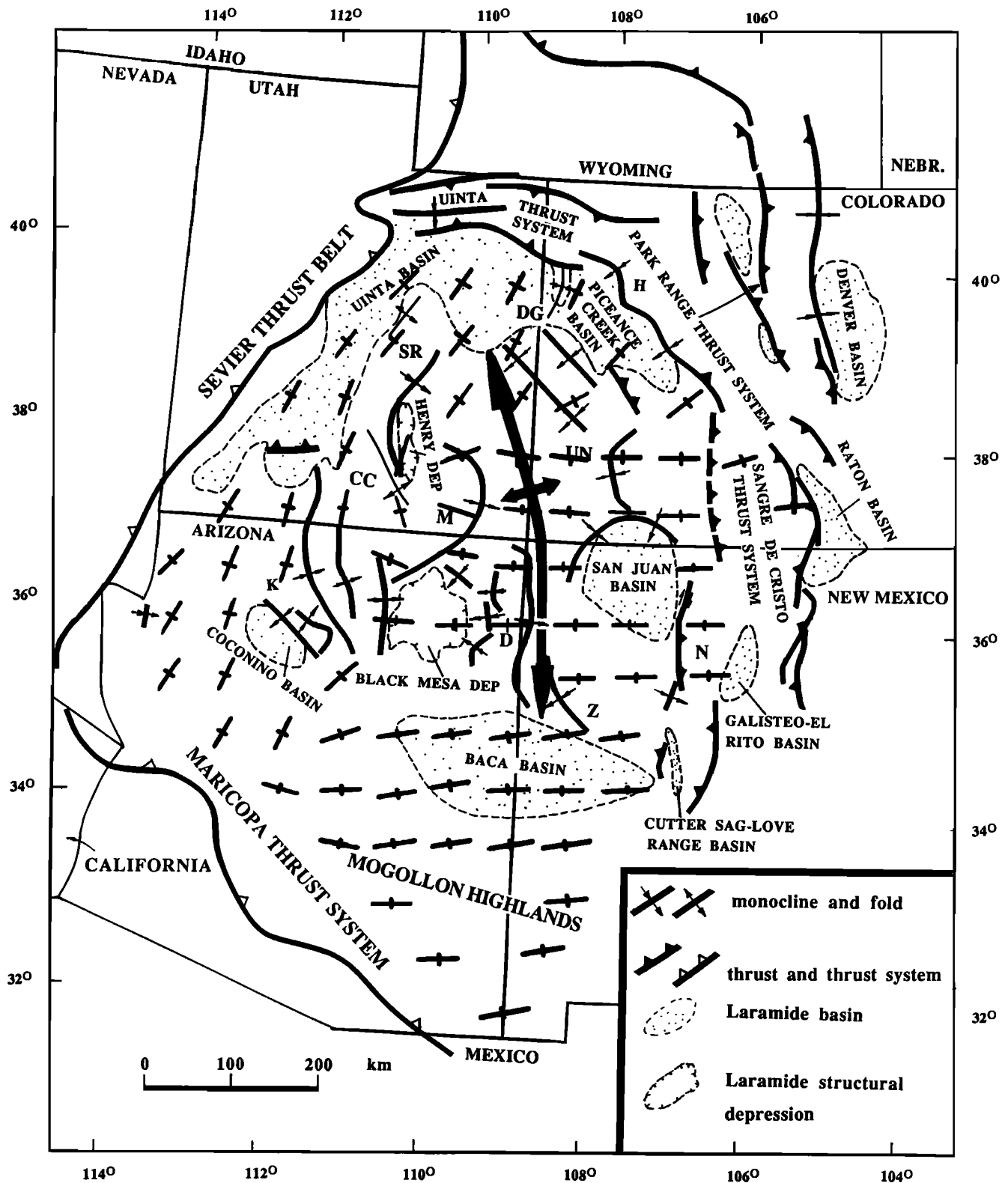


Figure 7. The principal stress trajectories obtained from computation shown in Figure 6 superposed on the Laramide structures in the Colorado Plateau region. Note that the fit is best in the northern, eastern, and southern parts of the plateau but is poor in the west central plateau.

only locally reported [e.g., Baltz, 1967]. The apparent kinematic discrepancy of the Uinta and the Park Range fault systems has been attributed to the interaction among the Uinta, Park Range, and Laramie Range fault systems on the northeastern corner of the Colorado Plateau region during

the Laramide orogeny [Yin *et al.*, 1992; Yin and Ingersoll, 1993].

The most interesting feature of the stress pattern shown in Figure 6 is that the greatest compressional direction in the northwestern part of the plate lies generally north-south.

This may explain the puzzling thrust systems recently discovered by *Lundin* [1989] and *Merle et al.* [1993] in southwestern Utah (Figure 7). Although these thrusts were interpreted to be related to mid-Tertiary magmatic emplacement that postdates the Laramide orogeny and predates Basin and Range extension, their poor age constraint (i.e., younger than the Eocene) in conjunction with the fact that the Laramide deformation in the southern Rocky Mountain region continued until the early Oligocene [*Dickinson et al.*, 1988], permits them to have been related to a complex stress field suggested in this study. The predicted principal stress directions match the geology poorly, however, in the west central plateau, where the N-S compressional belt is too wide.

The maximum magnitude of deviatoric stress is about 180 MPa, located in a narrow belt near the Uinta Mountains. This high stress magnitude is consistent with the unusually high friction required along this boundary. It implies that new fractures could have been created near this boundary under the boundary conditions defined here. Away from this boundary, the magnitude of deviatoric stress is quite low, mostly less than 50 MPa. The corresponding deflection pattern is a broad arch, consistent with the geologic observation.

### Evaluation of Model Parameters

In order to understand the properties of the thin plate model presented in this study, the effects of various model parameters are briefly discussed below. This allows us to assess the uniqueness of the best fit numerical simulation discussed above. The effect of the boundary faults on the stress distribution may be evaluated by varying their coefficients of friction ( $\mu_e^i$ ). Figure 8 shows directions of the principal stresses and the magnitude of deviatoric stress as a function of the effective coefficient of friction in the horizontal direction along the Sangre de Cristo thrust system, i.e.,  $\mu_e^3 = -0.08$  and  $-0.02$ . Other boundary conditions are defined as  $\mu_e^4 = -0.10$ ,  $\mu_e^5 = -0.10$ ,  $\alpha_1 = \alpha_2 = 1.1$ ,  $\beta_1 = \beta_2 = 1.0$ ,  $h = 15$  km,  $r = 2$  km, and  $(\rho_m - \rho_c) = 0.4$  gm/cm<sup>3</sup>. The values of  $\mu_e^3$ ,  $\mu_e^4$ , and  $\mu_e^5$  are all chosen to be small, because they are thrusts and might have had high pore fluid pressure along the fault zones during their development. The result of the simulations shows that the greatest principal stress direction (Figure 8a) is dominantly in the N-S and NW-SE directions for higher friction along the Sangre de Cristo fault system (i.e.,  $\mu_e^3 = -0.08$ , Figure 8a). As the friction decreases, the southwestern part of the plateau is dominated by NE-SW compression (i.e.,  $\mu_e^3 = -0.02$ ). The maximum magnitude of deviatoric stress decreases as the friction along the northern boundary decreases from 300 to 35 MPa (Figure 8b). However, the simulations cannot produce the simultaneous N-S compression in the Uinta Mountains and E-W compression along the eastern margin of the plateau.

Figure 9 shows the effect of different coefficients of friction along the northeastern boundary fault (the Park Range fault), i.e.,  $\mu_e^4 = 0.80$  and  $0.20$ . Other parameters used in the computation are the same as that in Figure 8, except  $\mu_e^3 = -0.10$  and  $\mu_e^5 = 0.10$ . The directions of greatest compression are mostly in the N-S and NW-SE directions (Figure 9a) for  $\mu_e^4 = 0.80$ . However, as  $\mu_e^4$  decreases to  $0.20$ , the directions of greatest compression lie in the E-W and NE-SW directions. In both situations, the simultaneous N-S compression along the northern boundary and the E-W

compression along the eastern boundary are not predicted. Furthermore, the maximum magnitude of deviatoric stress in both cases is unreasonably high, varying from 740 MPa for  $\mu_e^4 = 0.80$  to 140 MPa for  $\mu_e^4 = 0.20$  (Figure 9b). Deflection boundary conditions are assumed to be  $w_i = -0.5$  km,  $i = 1, 2, 3, 4, 5$ . The deflection pattern varies as  $\mu_e^4$  changes (Figure 9c). For  $\mu_e^4 = 0.80$ , the thin plate is depressed downward along its rim but is elevated in its central part to form a dome. For  $\mu_e^4 = 0.20$ , the northern part of the thin plate is depressed downward, whereas the southern part is uplifted into a broad dome. Comparison of the two cases suggests that deflection patterns are sensitive to the in-plane traction boundary conditions.

The magnitude of the regional stresses applied along the northwestern and southwestern boundaries is expressed by  $\alpha_1$ ,  $\alpha_2$ ,  $\beta_1$ , and  $\beta_2$ . Systematic evaluation of these parameters suggests that stress distributions and deflection patterns are very similar when  $\alpha_1$ ,  $\alpha_2$ ,  $\beta_1$ , and  $\beta_2$  are chosen between 1.1 and 1.4 and the principal stress direction applied along the western edge of the plateau varies within 20°.

It is possible that the loading along all sides of the plateau may not have occurred simultaneously. If this is the case, then a sequential loading condition may be applied. We find, however, that with the same total deflection along the boundary of the plateau, the resulted patterns are nearly identical, although their maximum amplitudes are slightly different.

In-plane horizontal compression and flexural loading along the edge of the thin plate may not be the only mechanism causing upward warping. It is possible that buoyancy could have been induced by an added crustal root, which in turn could have been produced by magmatic addition at the base of the crust below the Colorado Plateau. Because the approach adopted in this study is quasi-static, any vertical load, no matter how short its duration is, could have affected the mechanics of the plateau. We find that an added crustal root of less than 2 km thick in conjunction with loading by sediments and thrust sheets could have produced upward warping consistent with the observed geologic relationships.

### Complex Stress Distributions and Monoclinial Trends

Previous models attributed the various trends of monoclines on the Colorado Plateau to reactivation of pre-existing weakness under unidirectional compression [e.g., *Davis*, 1978]. This interpretation may have been reached because it was difficult to visualize why the stress field in the plateau should have been so different from the state of the regional stress. The model presented in this study is an end-member approach by assuming that the entire plateau region behaves as a coherent plate. It provides, in addition, a reasonable fit to the observed geology and thus a plausible physical basis of an alternative interpretation for the variable trends of the monoclines. The result of the numerical simulations shows that the state of the regional stress can differ significantly from the local stress field. For example, by changing the coefficients of friction along the boundary faults, the principal stress directions and magnitudes can change drastically from that of the assumed regional stress. Thus local structural trends not matching the regional compressional direction may not imply a kinematic incompatibility during structural development of a large region, a solution anticipated by *Kelley* [1955a] nearly 40 years ago.

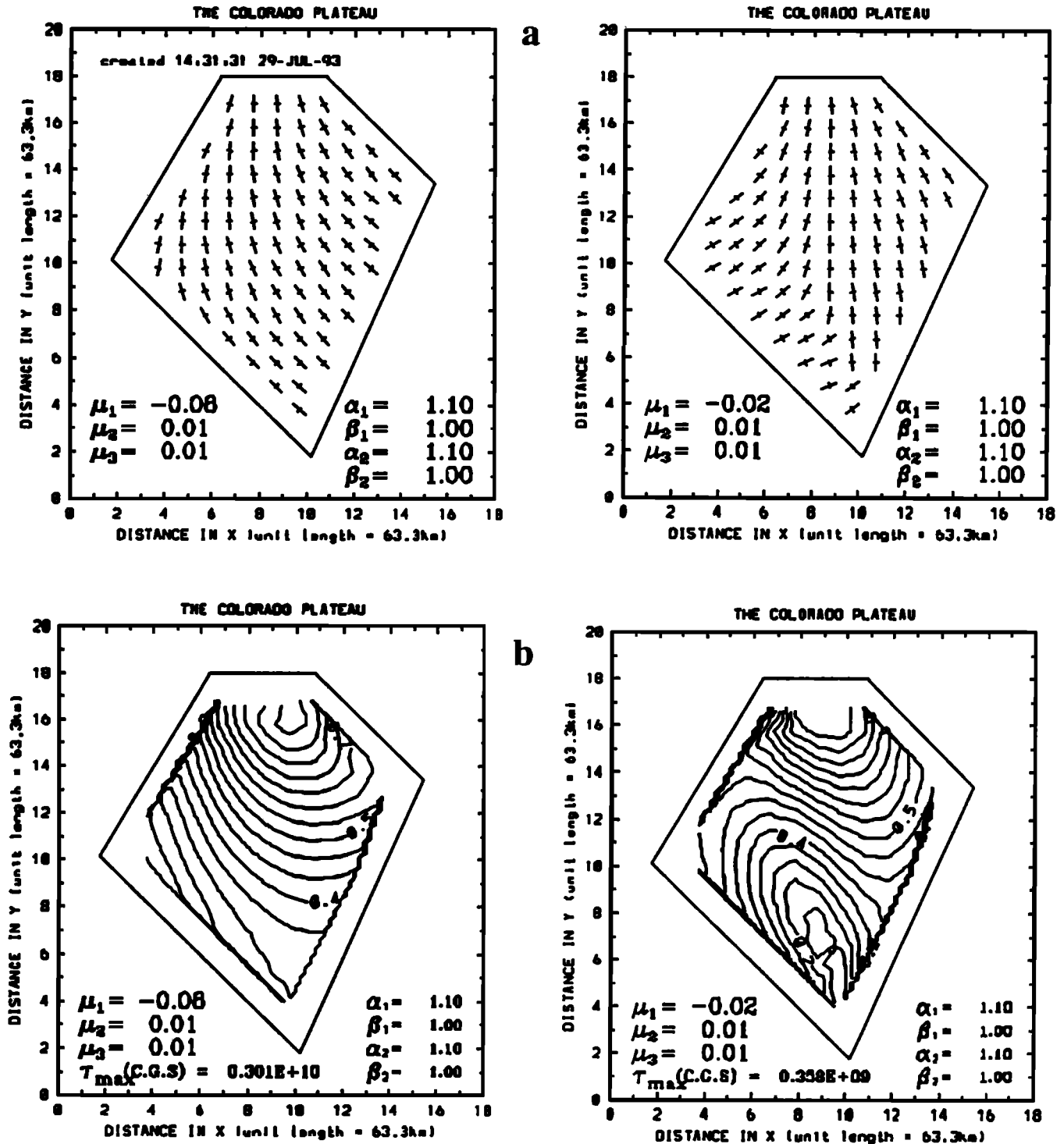


Figure 8. A simulation that does not fit the observed structures shown in Figure 1. See discussion in text. (a) Directions of the principal stresses and (b) the magnitude of deviatoric stress. The effective coefficient of friction along the southeastern boundary fault (the Sangre de Cristo thrust system) is assumed to be  $\mu_e^3 = -0.08$  and  $-0.20$ . Other parameters are  $\mu_e^4 = -0.10$ ,  $\mu_e^5 = -0.10$ ,  $h = 15$  km, and  $r = 2$  km.

## Conclusions

1. The Colorado Plateau region is a broad N-S trending arch developed during the Laramide orogeny. The development of warping was caused by a combination of horizontal

compression, buoyancy at the base of the crust, and loading by thrusting and sedimentation around the rim of the plateau. The resultant upward warping produced bending of the crust and thus shear stresses on the horizontal planes with a top-to-the-east shear on the west side and a top-to-the-west shear on the east side of the plateau. The subhori-

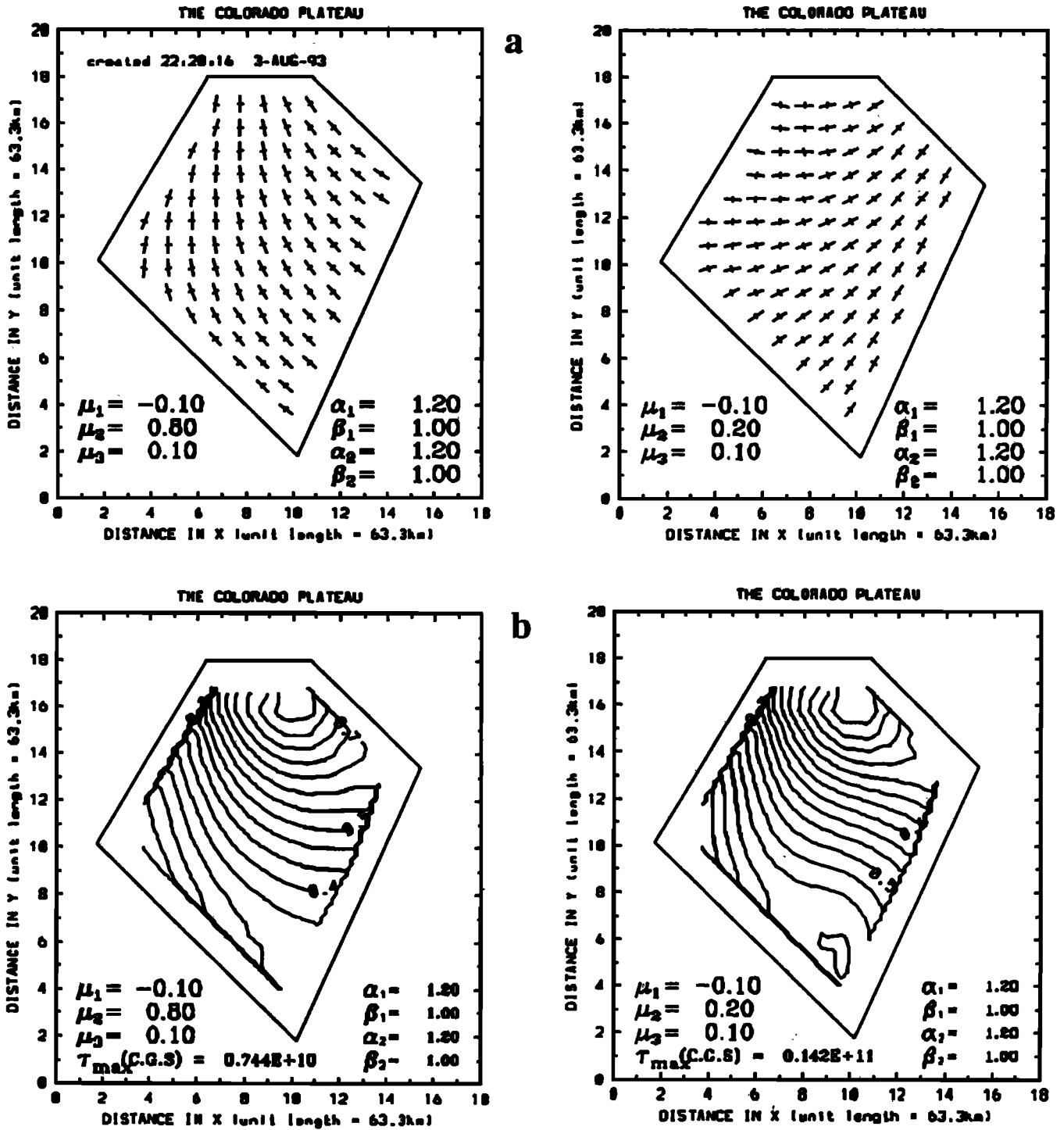


Figure 9. Another simulation that does not fit the observed structures shown in Figure 1. See discussion in text. (a) Directions of the principal stresses, (b) the magnitude of deviatoric stress, and (c) the deflection pattern of the thin plate, assuming  $\mu_e^4 = 0.80$  and  $0.20$ ,  $w_i = -0.5$ ,  $i = 1, 2, 3, 4, 5$ . Other parameters are the same as those used in the computation shown in Figure 8, except  $\mu_e^3 = -0.10$  and  $\mu_e^5 = 0.10$ .

zonal shearing in conjunction with the horizontal compression created the monoclines in the Colorado Plateau region that verge toward its center.

2. Variable trends of the monoclines in the Colorado Plateau region are produced by a stress field with variable directions of the principal stresses. This complex stress field

resulted from reactivation of preexisting, crustal-scale fault zones such as the Uinta fault, the Park Range-Front Range fault system, and the Nacimiento-Sangre de Cristo fault system. Stress distributions within the plateau region were highly sensitive to the coefficients of friction along these faults.

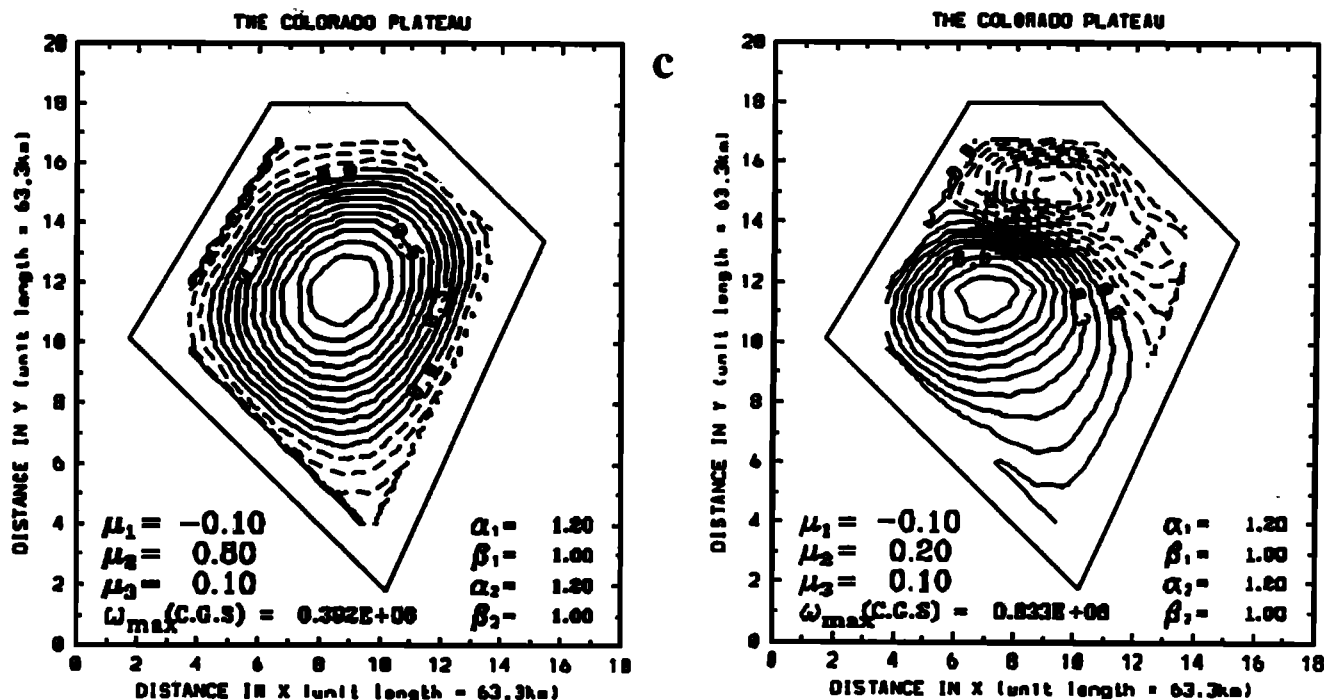


Figure 9. (continued)

3. The complex stress fields predicted by the thin plate model suggest that reactivation of pre-existing weakness within the plateau region does not have to be the sole reason for the formation of the variably trending monoclines.

4. A stress distribution that is compatible with both the trend of the monoclines and the overall warping pattern of the plateau requires that the coefficient of friction along the northern side of the plateau, i.e., the Uinta fault system, was at least 2 times greater than that along the northeastern and southeastern boundary faults. The lower inferred friction along the eastern side of the plateau may have been either related to the abnormally high pore fluid pressure along the Park Range and the Sangre de Cristo thrust systems, or to the low strength of the structures produced by the Ancestral Rocky Mountain orogeny. The latter reason may be more important, because the presence of salt (a low strength material) is common in the basins developed during the Ancestral Rocky Mountains orogeny.

**Acknowledgments.** The study was supported by the Academic Senate Research Fund from the University of California and partially by NSF grant EAR-9220105 awarded to An Yin. I am grateful to Philip Law for writing part of the plotting program. Reviews of a preliminary version of this manuscript by Donna J. Young and Liz Forshee are appreciated. I thank the JGR reviewers Dick Walcott, Ze'ev Reches, and Associate Editor Andrew Griscom for their constructive reviews that greatly improved the manuscript. This paper was written in memory of my dear friend, Kelly Ahlschwede.

## References

- Baker, A.A., Geologic structure of southeastern Utah, *AAPG Bull.*, 19, 1472-1507, 1935.
- Baltz, E.H., Stratigraphy and regional tectonic implications of part of Upper Cretaceous and Tertiary rocks, east-central San Juan basin, New Mexico, *U.S. Geol. Surv. Prof. Pap.*, 552, 101 pp., 1967.
- Beaumont, C., Foreland basins, *Geophys. J. R. Astron. Soc.*, 65, 291-329, 1981.
- Bernaski, G., Compressional Laramide deformation in the southeastern Uinta Mountains, northwestern Colorado, and northeastern Utah, M.S. thesis, Univ. of Wyo., Laramide, 1985.
- Burchfiel, B.C., and G.A. Davis, Mojave desert and environs, in *The Geotectonic Development of California*, edited by W.G. Ernst, pp. 218-252, Prentice-Hall, Englewood Cliffs, N. J., 1981.
- Byerlee, J., Friction of rocks, *Pure Appl. Geophys.*, 116, 615-626, 1978.
- Chapin, C.E., and S.M. Cather, Eocene tectonics and sedimentation in the Colorado Plateau-Rocky Mountain area, in *Rocky Mountain Foreland Basins and Uplifts*, edited by J.D. Lowell, pp. 33-56, Rocky Mountain Association of Geologists, Denver, Colo., 1983.
- Coney, P., Plate tectonics and the Laramide orogeny, *Spec. Publ. N. M. Geol. Soc.*, 6, 5-10, 1976.
- Davis, G.H., Monocline fold pattern of the Colorado Plateau, *Mem. Geol. Soc. Am.*, 151, 215-233, 1978.
- Davis, G.H., *Structural Geology of Rocks and Regions*, John Wiley, New York, 1985.

- Dewey, J.F., Nature and origin of kink-bands, *Tectonophysics*, *1*, 459-494, 1965.
- Dickinson, W.R., M.A. Klute, M.J. Hayes, S.U. Janecke, E.R. Lundin, M.A. McKittrick, and M.D. Olivares, Paleogeographic and paleotectonic setting of Laramide sedimentary basins in the central Rocky Mountain region, *Geol. Soc. Am. Bull.*, *100*, 1023-1039, 1988.
- Drewes, H., Development of the foreland zone and adjacent terranes of the Cordilleran orogenic belt near the U.S.-Mexico border, in *Interaction of the Rocky Foreland and the Cordilleran Thrust Belt*, edited by C.J. Schmidt and W.J. Perry, *Mem. Geol. Soc. Am.*, *171*, 447-463, 1988.
- Engebretson, D.C., A. Cox, and R.G. Gordon, Relative motions between oceanic and continental plates in the Pacific basin, *Spec. Pap. Geol. Soc. Am.*, *206*, 1-59, 1985.
- Fassett, J.E., Early Tertiary paleogeography and paleotectonics of the San Juan basin area, New Mexico and Colorado, in *Cenozoic Paleogeography of the Western Central United States, Rocky Mountain Paleogeography Symposium 3*, edited by R.M. Flores and S.S. Kaplan, pp. 317-334, Rocky Mountain Geologists Association, Denver, Colo. 1985.
- Fletcher, J.M., and K.E. Karlstrom, Late Cretaceous ductile deformation, metamorphism and plutonism in the Piute Mountains, eastern Mojave desert, *J. Geophys. Res.*, *95*, 487-500.
- Fung, Y.C., *Foundations of Solid Mechanics*, 593 pp., Chapman and Hall, New York, 1965.
- Gries, R.R., North-south compression of the Rocky Mountain foreland structures, in *Rocky Mountain Foreland Basins and Uplifts* edited by J.D. Lowell, pp. 9-32, Mountain Geologists, Denver, Colo., 1983.
- Grout, M.A., G.A. Abrams, R.L. Tang, T.J. Hainworth, and E.R. Verbeek, Late Laramide thrust-related and evaporite-domed anticlines in the southern Piceance Basin, northeastern Colorado, *AAPG Bull.*, *75*, 205-218, 1991.
- Hansen, W.R., Geology of the Flaming Gorge area, Utah-Colorado-Wyoming, *U.S. Geol. Surv. Prof. Pap.*, *490*, 196 pp., 1965.
- Hubbert, M.K., and W.W. Rubey, Role of fluid pressure in mechanics of overthrust faulting, I, Mechanics of fluid-filled porous solids and its applications to overthrust faulting, *Geol. Soc. Am. Bull.*, *70*, 115-166, 1959.
- Jaeger, J.C., and N.G.W. Cook, *Fundamentals of Rock Mechanics*, 93 pp., Chapman and Hall, New York, 1979.
- Johnson, R.C., Early Cenozoic history of the Uinta and Piceance Creek basins, Utah and Colorado, with special reference to the development of Eocene Lake Uinta, in *Cenozoic Paleogeography of the Western Central United States*, , edited by R.M. Flores and S.S. Kaplan, pp. 247-276, Rocky Mountain Geologists Association, Denver, Colo., 1985.
- Jordan, T.E., Thrust loads and foreland basin evolution, Cretaceous, western United States, *AAPG Bull.*, *65*, 2506-2520, 1981.
- Kelley, V.C., Monoclines of the Colorado Plateau, *Geol. Soc. Am. Bull.*, *66*, 789-804, 1955a.
- Kelley, V.C., Regional tectonics of the Colorado Plateau and relationship to the origin and distribution of Uranium, *Publ. Geol.* *5*, 120 pp., University of N. M., Albuquerque, 1955b.
- King, P.B., and H.M. Beikman, Geologic map of the United States, scale 1:1,500,000, U.S. Geol. Surv., Reston, Va., 1974.
- Lundin, E.R., Thrusting of the Claron Formation, the Bryce Canyon region, Utah, *Geol. Soc. Am. Bull.*, *101*, 1038-1050, 1989.
- Mount, V.S., and J. Suppe, Present-day stress orientation adjacent to strike-slip faults: California and Sumatra, *J. Geophys. Res.*, *97*, 11995-12013, 1992.
- Merle, O.R., G.H. Davis, R.P. Nickelsen, and P.A. Gourlay, Relation of thin-skinned thrusting of Colorado Plateau strata in southwestern Utah to Cenozoic magmatism, *Geol. Soc. Am. Bull.*, *105*, 387-398, 1993.
- Nation, D., J.C. Wilt, and R.H. Hevly, Cenozoic stratigraphy of Arizona, in *Cenozoic Paleogeography of the Western Central United States, Rocky Mountain Paleogeography Symposium 3*, edited by R.M. Flores and S.S. Kaplan, pp. 335-356, Rocky Mountain Geologists Association, Denver, Colo., 1985.
- Quinlin, G.M., and C. Beaumont, Appalachian thrusting, lithospheric flexure, and the Paleozoic stratigraphy of the eastern interior of North America, *Can. J. Earth Sci.*, *21*, 973-996, 1984.
- Reches, Z., Development of monoclines, I, Structure of the Palisades Creek branch of the East Kaibab monocline, Grand Canyon, Arizona, in *Laramide Folding Associated with Basement Block Faulting in the Western United States* edited by V. Matthews III, *Mem. Geol. Soc. Am.*, *151*, 235-271, 1978.
- Reches, Z., and A.M. Johnson, A theory of concentric, kink and sinusoidal folding and of monoclinical flexuring of compressible, elastic multilayers, VI, Asymmetric folding and monoclinical kinking, *Tectonophysics*, *32*, 295-320, 1976.
- Reches, Z., and A. M. Johnson, Development of monoclines, II, Theoretical analysis of monoclines, in *Laramide Folding Associated with Basement Block Faulting in the Western United States* edited by V. Matthews, III, *Mem. Geol. Soc. Am.*, *151*, 273-313, 1978.
- Ryder, R.T., T.D. Fouch, and J.H. Elison, Early Tertiary sedimentation in the western Uinta Basin, Utah, *Geol. Soc. Am. Bull.*, *87*, 496-512, 1974.
- Sinclair, H.D., B.J. Coakley, P.A. Allen, and A.B. Watts, Simulation of foreland basin stratigraphy using a diffusion model of mountain belt uplift and erosion: An example from the central Alps, Switzerland, *Tectonics*, *10*, 599-620, 1991.
- Smith, L.N., S.G. Lucas, and W.E. Elston, Paleogene stratigraphy, sedimentation and volcanism of New Mexico, in *Cenozoic Paleogeography of the Western Central United States, Rocky Mountain Paleogeography Symposium 3*, edited by R.M. Flores and S.S. Kaplan, pp. 293-316, Rocky Mountain Geologists Association, Denver, Colo., 1985.
- Tweto, O., Laramide (Late Cretaceous to Early Tertiary) orogeny in the southern Rocky Mountains, *Mem. Geol. Soc. Am.*, *144*, 1-44, 1975.
- Wang, Q.M., T. Nishidai, and M.P. Coward, The Tarim basin, NW China: Formation and aspects of petroleum geology, *J. Pet. Geol.*, *15*, 5-34, 1992.
- Wernicke, B., Uniform-sense normal shear of the continental

- lithosphere, *Can. J. Earth Sci.*, *22*, 108-125, 1985.
- Yin, A., Mechanisms for the formation of domal and basinal detachment faults: A three-dimensional analysis, *J. Geophys. Res.*, *96*, 14,577-14,594, 1991.
- Yin, A., and R.V. Ingersoll, Tectonic development of Laramide thrusts and basins in southern U.S. Rocky Mountains, *Geol. Soc. Am. Abstr. Programs*, *25*, 167, 1993.
- Yin, A., E.D. Paylor II, and A. Norris, Analysis of Laramide crustal strain distribution using relative-slip circuits, *Geol. Soc. Am. Abstr. Programs*, *24*, 69, 1992.
- 
- A. Yin, Department of Earth and Space Sciences, University of California, Los Angeles, CA 90024-1567.
- (Received August 23, 1993; revised May 13, 1994; accepted May 18, 1994.)